

Article

Human-like Trajectory Planning for Autonomous Vehicles Using Flexible Virtual Reference Points in Car Overtaking Motorcycle Scenarios

Sitthichok Sitthiracha^{1,a}, Chinnawut Nantabut^{1,b,*}, Saiprasit Koetnuyom^{1,c},
and Gridsada Phanomchoeng^{2,d}

¹ Sirindhorn International Thai-German Graduate School of Engineering, King Mongkut's University of Technology North Bangkok, 1518 Pracharat 1 Road, Wongsawang, Bangsue, Bangkok, 10800, Thailand

² Department of Mechanical Engineering, Faculty of Engineering, Chulalongkorn University, 254 Phayathai Road, Wangmai, Pathumwan, Bangkok 10330, Thailand

E-mail: ^abirdyossr@gmail.com, ^{b,*}chinnawut.n@tggs.kmutnb.ac.th (Corresponding author),

^csaiprasit.k@tggs.kmutnb.ac.th, ^dgridsada.phanomchoeng@gmail.com

Abstract. Traditionally, autonomous vehicles (AVs) prioritize safety and efficiency when planning trajectories. However, the lack of human-like driving behaviors can limit user trust and acceptance. This can be attributed to difficulties in communication and interpreting the intentions of other road users, particularly during interactions like overtaking maneuvers. This study proposes the Flexible Virtual Reference Point (FVRP) concept, an enhancement to model-based trajectory planning that facilitates human-like behavior during overtaking maneuvers. FVRP decomposes complex overtaking maneuvers into distinct phases. Within each phase, the concept strategically positions virtual reference points by considering both driver comfort data and prevailing traffic constraints. These reference points are then connected to form a piecewise trajectory, ensuring the optimization of both safety and comfort during overtaking maneuvers involving a motorcycle (MC). The results demonstrate that FVRP successfully generates trajectories that achieve both safety and driver comfort across all experimental settings. Furthermore, the trajectories generated by FVRP exhibit characteristics that resemble human drivers, while maintaining safe and comfortable distances compared to those generated by driver behavior models and optimal control models. The success of FVRP concept in car-to-MC overtaking maneuvers suggests its potential for adaptation to other driving maneuvers where comfort and safety need to be balanced.

Keywords: Driver comfort, human-like trajectory planning, motorcycle overtaking safety, overtaking maneuvers, virtual reference points.

ENGINEERING JOURNAL Volume 28 Issue 10

Received 29 May 2024

Accepted 18 October 2024

Published 31 October 2024

Online at <https://engj.org/>

DOI:10.4186/ej.2024.28.10.77

1. Introduction

Safe and efficient autonomous driving necessitates a focus on both technical capabilities and human factors [1]. A critical component of achieving this goal is trajectory planning, where AVs determine their trajectories through the environment. While traditional approaches prioritize metrics like collision avoidance and efficiency, there's a growing interest in human-like trajectory planning, aiming to mimic the way humans navigate complex dynamic environments.

Extensive research has been conducted on identifying feasible and optimal paths or trajectories for AVs [2-4]. These methods aim to ensure collision avoidance with other vehicles and obstacles and include techniques like graph search, incremental search, sampling-based algorithms, potential fields, cell decomposition, numerical optimization, and curve interpolation.

Several studies have explored integrating driver characteristics into human-like trajectory planning. For instance, Dai et al. [5] proposed an optimal lane-change trajectory using road coordinate system and driver data. Their approach achieved human-likeness by considering lane-changing time and the slope of lane-changing trajectory. Similarly, Naidja et al. [6] employed clothoid interpolation for generating human-like trajectories at unsignalized intersections, while optimizing the path with a particle swarm optimizer. Other studies leveraged machine learning techniques: Zhao et al. [7] developed a preview-based model for negotiating curves using long short-term memory networks trained on driver data, and Nan et al. [8] utilized deep inverse reinforcement learning to generate data-driven trajectories for merging scenarios. Additionally, Liu et al. [9] implemented maximum entropy inverse reinforcement learning to model driver intention for left turns at unsignalized intersections. Furthermore, Fajen and Jansen [10] proposed a non-model approach using forward waypoints, and Cui et al. [11] presented a constraint-imitative method combining artificial potential fields and dynamic movement primitives. Notably, Chen et al. [12] proposed transforming the lane-change problem into a two-dimensional car-following problem.

While safety remains a primary focus, with all these studies prioritizing collision avoidance, none explicitly consider human factors like driver comfort distances within the trajectory planning process. This omission of human factors might negatively impact user trust and ultimately hinder AV acceptance [13]. Conversely, research suggests that incorporating driver characteristics into trajectory planning is crucial for improving user acceptance of AVs [14].

Comfort is a key concept in human factors, impacting how people experience a system or environment. It is a complex and subjective feeling encompassing both positive (enjoyment) and negative (anxiety) aspects [15-16]. Traditionally, car ergonomics focused on physical comfort factors like seat vibration, noise, and temperature [17]. However, in AVs, the driver's experience goes beyond

ergonomics due to the lack of driver control. While recent research has addressed other driver physical comfort by incorporating constraints like jerk and acceleration [18-20], a crucial question remains unanswered: what is the ideal vehicle-to-vehicle distance gap for driver in AVs to feel safe and comfortable?

By incorporating driver-preferred following distances into trajectory planning, human comfort levels can be improved [21]. Studies have investigated the gap acceptance chosen by drivers in various interactions, such as car-to-bicycle, car-to-pedestrian, and car-to-MC [13, 22-24]. However, existing trajectory planning in AVs does not explicitly consider driver psychological comfort. This rich data offers an opportunity to enhance model-based trajectory planning with more human-like behaviors.

This study aims to bridge the gap between model-based trajectory planning and quantitative driver comfort zone by introducing the Flexible Virtual Reference Point (FVRP) approach. The constraints employed within this model will be derived from both driver comfort distance thresholds and traffic safety criteria.

The key contribution of FVRP concept is enhancing model-based trajectory planning by decomposing complex overtaking maneuvers into distinct phases. Virtual reference points are then strategically positioned within each phase, considering both driver comfort data and prevailing traffic safety constraints. These reference points are subsequently connected to form a piecewise trajectory. This approach aims to preserve human-like driving behavior while ensuring adherence to safety.

Prior to AV execution of the overtaking maneuver, a crucial safety check is implemented to guarantee safety. This verification process, which is another key contribution, utilizes the total longitudinal distance required for the entire maneuver.

This work is structured as follows. Section 2 details the formulation of the car overtaking MC problem, the planning algorithm for coordinate assignment, trajectory generation, and the safety check condition. Section 3 presents the experimental results and analyzes the effectiveness of the proposed concept. Section 4 concludes the paper.

2. Materials and Methods

2.1. Psychology of Driving

Driving can be conceptualized as a dynamic control process that demands constant adaptation to changing environmental conditions to achieve desired outcomes [25-26]. This aligns with the concept of task control, which involves managing and directing actions to maintain desired states despite external disturbances. Humans, as biological control systems, possess an inherent ability to execute this control function effectively while driving.

Traditional driving models often prioritize task execution over the underlying motivations influencing driver behavior and performance [27]. Michon's hierarchical framework illustrates how high-level goals,

such as lane changes, guide lower-level control actions [28]. However, this model does not explain the origins of these high-level goals. Motivational theories attempt to fill this gap by identifying factors such as risk perception, tolerance, and avoidance [29-31] as key determinants of driver behavior.

Driver motivation significantly influences the selection of control task reference values. Discomfort, perceived as an immediate threat, can override abstract risk assessments, prompting drivers to prioritize safety [29, 31]. Ideally, drivers aim to balance task accomplishment with maintaining a psychological comfortable state, avoiding situations that could potentially lead to accidents or loss of control. This desired state of comfort and safety defines a 'comfort zone' within which drivers prefer to operate. For example, in a pedestrian overtaking scenario, the driver needs to maintain a safe lateral distance while overtaking, but this distance can vary depending on the presence of oncoming traffic as shown in Fig. 1. The term "comfort zone" in this study specifically denotes the psychological distance drivers prefer to maintain, rather than the physical comfort of passengers as defined by ISO 2631 concerning vertical vibration.

2.2. Problem Formulation

Figure 2 illustrates the car overtaking MC scenario, considering left-hand traffic conventions as in Thailand. The ego vehicle (the vehicle with the control system) approaches a slower MC and needs to overtake under free traffic conditions. When a pre-defined following distance is reached, and the MC's speed is significantly lower than the ego vehicle's intended cruising speed, the system initiates the overtaking maneuver, assuming right-hand overtaking is permitted.

The car overtaking MC maneuver can be defined using the four-phase model. As the ego vehicle approaches the MC from behind, Phase 1 (approaching) begins. This phase ends when the system decides to initiate a lane change for overtaking. Phase 2 (steering away) starts when the ego vehicle maneuvers laterally away from the MC and ends when it returns to a straight-line trajectory. Phase 3 (passing) allows the ego vehicle to safely pass the MC. Finally, Phase 4 (returning) begins when the ego vehicle steers back to its original lane position. This four-phase model provides a framework for applying the FVRP approach to generate human-like and comfortable overtaking trajectories.

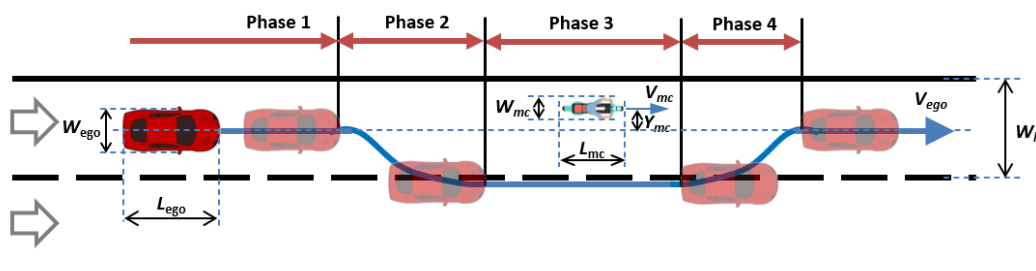


Fig. 2. Four phases of the car overtaking motorcycle maneuver.

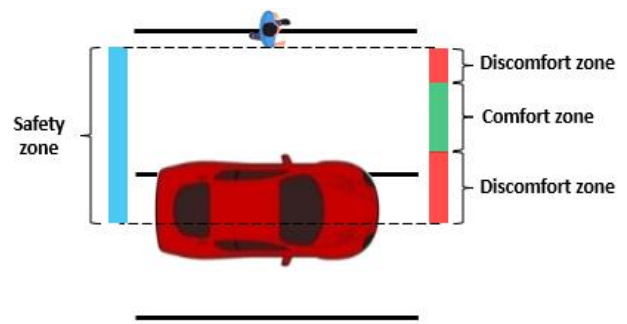


Fig. 1. Sample of comfort zone in car overtaking a pedestrian adapted from [23].

Before initiating the overtake maneuver, the following conditions are likely to be met:

- The overtaken MC is traveling in a straight line.
- The velocity of the overtaken MC (V_{mc}) is known, steady, and less than the ego vehicle speed (V_{ego}).
- The lateral position of the overtaken MC (Y_{mc}) relative to the center of the left lane is known
- The lane width (W_l) is known.
- The dimensions of both the ego vehicle (L_{ego} and W_{ego}) and the MC (L_{mc} and W_{mc}) are known.
- Real-time information about the relative position between the vehicles is available from onboard sensors.

2.3. Overtaking Maneuver Data Collection

To quantify driver comfort zones, specific gap measurements were defined around MC as shown in Fig. 3: Gap_1 and Gap_2 for the longitudinal distance between MC and the following vehicle during Phase 1 and 2, Gap_{Lat} for the lateral distance during the parallel phase, and Gap_3 and Gap_4 for the longitudinal distance between the vehicles during Phase 3 and 4. These longitudinal gaps, excluding Gap_{Lat} , were calculated using time-to-collision metrics as shown in Eq. (1).

$$TTC_1 = \frac{Gap_i}{\Delta V} \quad (1)$$

where $i \in \{1, 2, 3, 4\}$ indicates the phase in which TTC is calculated; Gap_i is the longitudinal distance in each phase as defined in Fig. 3, and ΔV is the speed difference between the leading and following vehicles.

A driving simulation experiment was conducted using a high-fidelity simulator at Smart Mobility Research Center, Chulalongkorn University equipped with a six-degree-of-freedom motion platform and immersive

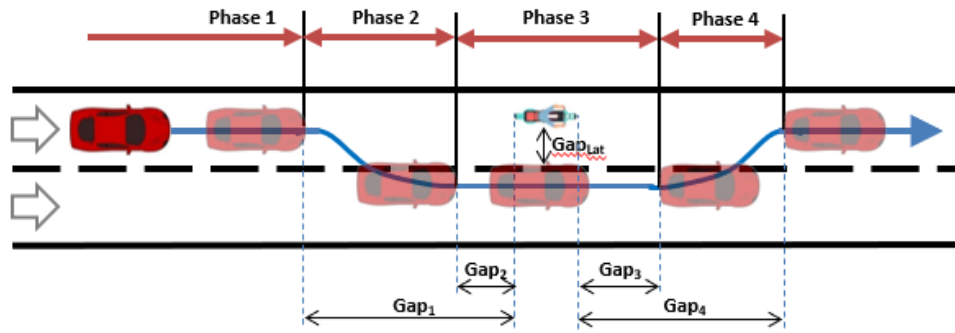


Fig. 3. Comfort distances around MC.

visuals displayed on three screens as shown in Fig. 4. The study simulated overtaking maneuvers on a four-lane, left-hand traffic urban road with a central median. The dimensions of the simulated motorcycle and test vehicle were 0.84 by 2.10 m and 1.83 by 4.58 m, respectively. 36 Thai participants, with an average age of 36.3 years and at least five years of driving experience, volunteered to take part in the experiment. After obtaining informed consent and completing a simulator familiarization process, participants were instructed to perform overtaking maneuvers at their preferred speeds. They were allowed to take breaks as needed throughout the experiment.

A series of driving scenarios were created to investigate the impact of motorcycle speed and position on overtaking behavior. Motorcycle speeds were set at 20, 40, and 60 km/h, while lateral positions ranged from -1 to 1.5 m in 0.5-m increments relative to the lane center. A total of 18 different scenarios were simulated, resulting in 648 data sets when considering the number of participants.

The simulated driving environment featured only the test vehicle and MC, creating an isolated overtaking scenario. Once the driver approached the simulated motorcycle, they initiated the overtaking maneuver. The driver's steering wheel angle, velocity, and vehicle speed were recorded at a sampling rate of 0.1 seconds throughout the overtaking process.



Fig. 4. Driving simulator.

2.4. Overtaking Maneuver Modelling

The overtaking maneuvers were analyzed to inform trajectory planning. The maneuver was divided into sequential stages [32], similar to a double lane change as shown in Fig. 5. Steering wheel velocity was initially considered for phase identification but was found to be unreliable due to driver variability [33]. To address this, steering wheel velocity data was simplified into a three-level system (-1, 0, 1) to accurately define the start and end of each overtaking phase as shown in Fig. 5.

Following phase identification, regression models were developed to analyze the relationship between comfort zone parameters and motorcycle lateral position (Y_{mc}) suggested in the study [24], as presented in Eq. (2) to (6).

$$TTC_1 = 1.04Y_{mc} + 7.12 \tag{2}$$

$$TTC_2 = 0.28Y_{mc} + 1.59 \tag{3}$$

$$Gap_{Lat} = -0.31Y_{mc} + 0.95 \tag{4}$$

$$TTC_3 = 0.29 \log_e(Y_{mc} + 1.5) \tag{5}$$

$$TTC_4 = -0.46Y_{mc} + 5.2 \tag{6}$$

where $-1.5 \leq Y_{mc} \leq 1.5$

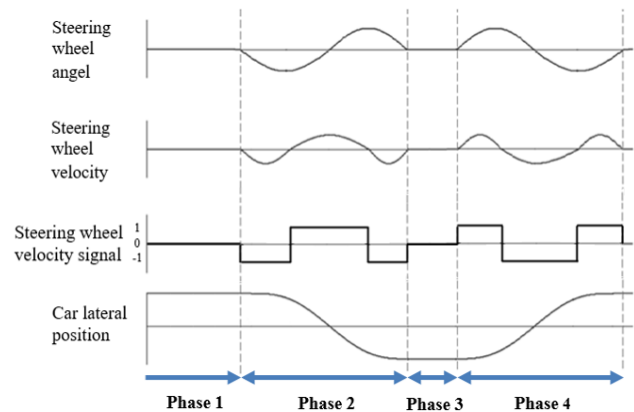


Fig. 5. Ideal time course of double-lane change maneuver and steering wheel velocity signal transformation.

The vehicle's trajectory was also modelled as a segmented path consisting of four distinct sections aligned with the overtaking maneuver phases as depicted in Fig. 5. While Phase 1 and 3 were represented as straight lines, Phase 2 and 4 were modelled using polynomial curves representing average trajectories of the data as shown in Fig 6 to 7 becoming Eq. (7) to (8) respectively.

$$Y_{ph2} = 3.2x^2 - 2.2x^3 \quad (7)$$

$$Y_{ph4} = 1 - 0.2x - 2.7x^2 + 2x^3 \quad (8)$$

2.5. Trajectory Planner Design Using Virtual Reference Points with Driver Comfort Zones and Safety Constraints

Prior to initiating the overtaking maneuver, a reference trajectory is generated for the ego vehicle. This planning method utilizes virtual reference points strategically positioned relative to MC. These points offer flexibility by adapting to both quantified driver comfort data and established traffic safety constraints.

The core function of the planner involves comparing the quantified driver comfort distances (TTC_1 , TTC_2 , Gap_{Lat} , TTC_3 , and TTC_4) against established safety criteria detailed in Table 1. A potential safety concern arises in Phase 3, as highlighted in the study [24]. Drivers typically maintain a smaller lateral gap between the ego vehicle and MC during this phase. There is currently no international standard for a safe passing gap. While some countries have specific regulations, there is a lack of uniformity. Thailand

and Japan lack legislation on minimum safe gaps when passing cyclists or motorcyclists. Some US states have adopted a "three-foot law". Certain European countries mandate a minimum clearance of 1.5 m. Australia uses a tiered system: 1 m for passing speeds up to 60 km/h and 1.5 m for speeds exceeding 60 km/h [36]. Due to the lack of a universal standard and the observed driver behavior in Phase 3, this study adopts the Australian safety criteria [36] as it represents a balanced approach among the existing regulations.

To achieve a balance between safety and the lateral comfort distances, the planner optimizes the distance between the side of the MC and the side of the ego vehicle (Gap_{Opt}) using Eq. (9).

$$Gap_{Opt} = \max(Gap_V, Gap_{Lat}) \quad (9)$$

$$\text{where } Gap_V = \begin{cases} 1, & V_{ego} \leq 60 \text{ km/h} \\ 1.5, & V_{ego} > 60 \text{ km/h} \end{cases}$$

The larger value between Gap_{Lat} and Gap_V is chosen for Gap_{Opt} . In simpler terms, if the safety criterion dictates a larger gap than the driver's comfort distance, Gap_{Opt} prioritizes safety by adopting the Gap_V value (which can be either 1 m or 1.5 m based on the Australian standards). This may necessitate the ego vehicle to move laterally further to create a safe gap during overtaking. The Gap_{Opt} value calculated from Eq. (9) is then used to modify driver comfort distances in subsequent equations which define the reference points P1 to P4 guiding the ego vehicle's trajectory during the overtaking maneuver as depicted in Fig. 8 as follows.

2.5.1 Point P1

The first virtual reference point, P1, defines the ego vehicle's desired position at the conclusion of Phase 1. This point is strategically located at the center of the lane (0 m lateral distance) with a longitudinal distance determined by TTC_1 associated with Phase 1. To achieve a balance between ensuring safety and maintaining driver comfort, Eq. (2) is modified by incorporating the Gap_{Opt} calculated from Eq. (9). The modified equation is presented below.

$$TTC_1 = 1.04(Y_{mc} + Gap_{Opt} - Gap_{Lat}) + 7.12 \quad (10)$$

Table 1. Traffic safety criteria for overtaking maneuvers.

Parameters	Criteria	References
TTC_1	$\geq 4s$	[34]-[35]
TTC_2	-	
Gap_{Lat}	≥ 1.0 m up to 60 km/h ≥ 1.5 m above 60 km/h	[36]
TTC_3	$\geq 0s$	[37]
TTC_4	-	

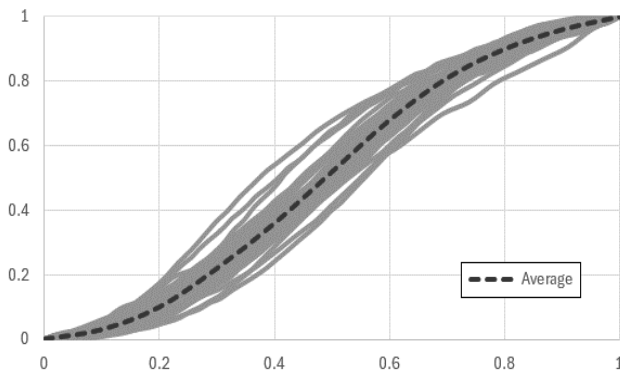


Fig. 6. Normalized steering curves in Phase 2.

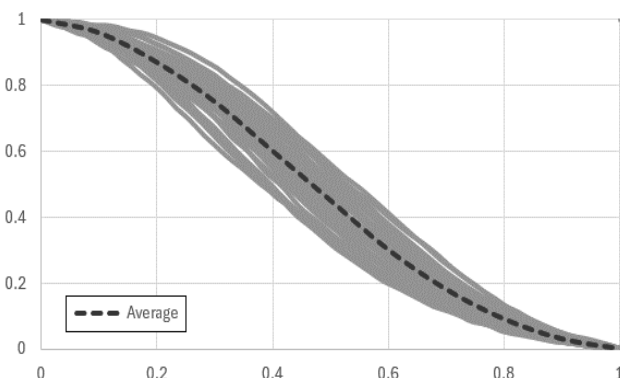


Fig. 7. Normalized steering curves in Phase 4.

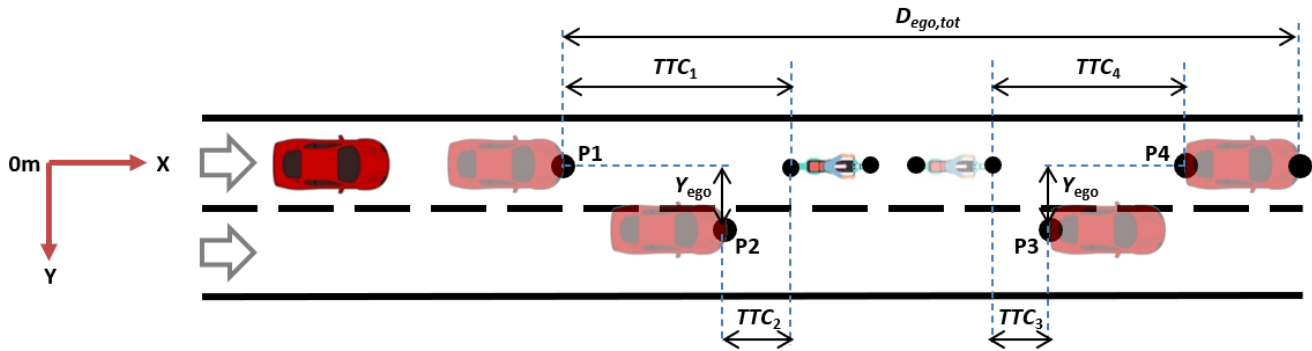


Fig 8. Schematic of virtual reference points in overtaking maneuver.

2.5.2 Point P2

The second virtual reference point, P2, defines the ego vehicle's desired position at the end of Phase 2. This point is determined by both its longitudinal and lateral displacements. The lateral position of P2 is defined by the ego vehicle's lateral offset (Y_{ego}) in m, as calculated in Eq. (11). This offset value dictates the lateral movement of the ego vehicle away from MC during Phase 2.

$$Y_{ego} = \min(Y_{mc} + Gap_{Opt} + \frac{W_{ego} + W_{mc}}{2}, W_l) \quad (11)$$

where W_{ego} = ego car width in m, W_{mc} = MC width in m, W_l = lane width in m.

The lateral offset of the ego vehicle Y_{ego} at point P2 is critical for safe lane utilization during overtaking. A crucial safety check is also implemented: if the calculated Y_{ego} exceeds the lane width W_l , it is capped at W_l . This ensures that the ego vehicle's lateral movement remains within the designated lane and avoids potentially encroaching on oncoming traffic or a physical traffic island in the case of a four-lane road.

Similar to P1, the longitudinal distance of P2 is based on the TTC_2 associated with Phase 2. To achieve the optimal balance between safety and comfort distances, Eq. (3) is modified by incorporating the Gap_{Opt} value obtained from Eq. (9). The resulting modified equation is presented below.

$$TTC_2 = 0.28(Y_{mc} + Gap_{Opt} - Gap_{Lat}) + 1.59 \quad (12)$$

2.5.3 Point P3

The third virtual reference point, P3, defines the desired position of the ego vehicle at the end of Phase 3. Similar to P2, its location is determined by both longitudinal and lateral components. P3 inherits the lateral offset Y_{ego} calculated in Eq. (11). This offset maintains a consistent lateral distance between the ego vehicle and MC throughout Phases 2 and 3.

Unlike P1 and P2, P3 utilizes the quantified driver comfort TTC_3 value associated with Phase 3. As noted in the study [24], TTC_3 values typically range from -0.4 to 0.4 s. While there is no established safety standard for TTC_3 in the context of overtaking a slower motorcycle [37], a

value of zero seconds might be considered acceptable. However, to prioritize rider comfort and avoid aggressive maneuvers during overtaking, this study adopts a fixed buffer of 0.4 s for TTC_3 . This choice is made in the absence of specific research on motorcyclist perception during overtaking maneuvers. Additionally, this value remains within the range of driver comfort identified in the study [24].

2.5.4 Point P4

Finally, the fourth virtual reference point, P4, is positioned in line with the lane center (0 m lateral distance) and utilizes an optimum TTC_4 . To achieve the optimal balance between safety and comfort distances, Eq. (6) is modified by incorporating the Gap_{Opt} value obtained from Eq. (9). The resulting modified equation is presented below.

$$TTC_4 = -0.46(Y_{mc} + Gap_{Opt} - Gap_{Lat}) + 5.2 \quad (13)$$

In conclusion, the positions of P1 to P4 are summarized in Table 2.

Table 2. Positions of virtual reference points P1 to P4.

Point	Positions	
	Longitudinal (s)	Lateral (m)
P1	TTC_1	0
P2	TTC_2	Y_{ego}
P3	$TTC_3 = 0.4$	Y_{ego}
P4	TTC_4	0

2.6. Decision Making Conditions to Engage Overtaking Maneuver

Following the assignment of reference point coordinates (P1-P4), a critical safety check is performed to ensure the ego vehicle can execute the overtaking maneuver safely. This verification process utilizes the total longitudinal distance required for the entire maneuver ($D_{ego,tot}$) as defined in Eq. (14). Essentially, $D_{ego,tot}$ represents the minimum free space needed for the ego vehicle to complete the overtaking maneuver within the lane boundaries as shown in Fig. 2.

$$D_{ego,tot} = V_{ego} \left(\frac{TTC_1 + TTC_4}{3.6} + \frac{L_{ego} + L_{mc}}{V_{ego} - V_{mc}} \right) \quad (14)$$

where V_{ego} = ego vehicle speed in km/h, V_{mc} = MC speed in km/h, L_{ego} = ego car length in m, L_{mc} = MC length in m.

The planner compares the ego vehicle's front headway (available longitudinal distance in front of the ego vehicle) with $D_{ego,tot}$. If the front headway is greater than $D_{ego,tot}$, it indicates sufficient space for safe overtaking, and the maneuver can proceed. Conversely, if the front headway is less than $D_{ego,tot}$ (i.e., insufficient space), the ego vehicle must maintain its position behind MC to avoid a collision. This prioritizes safety by ensuring the ego vehicle only attempts overtaking when there's adequate space within the traffic flow.

2.7. Trajectory Generation for Overtaking Maneuver

Once the planner confirms the overtaking maneuver's feasibility (sufficient space available), the trajectory for the ego vehicle is generated. This trajectory planning utilizes a piecewise approach, where a two-point boundary value problem is solved at each relevant time step. This iterative process ensures the generated trajectory adheres to the defined reference points (P1-P4) and adheres to safety and comfort considerations throughout the overtaking maneuver.

2.7.1 Piecewise trajectory between point P1 and P2

Following the definition of reference point P1 and P2 in Phase 2, a smooth geometric curve is required to connect them, ensuring a comfortable and controlled overtaking maneuver. Eq. (7) was used to construct a piecewise trajectory between P1 and P2. This specific polynomial is modified to be Eq. (15) - (17) with constant ego vehicle speed (V_{ego}). This approach ensures a natural transition between the initial and intermediate overtaking stages.

$$x_{Ph2}(t) = \frac{V_{ego}}{3.6} t, \quad 0 \leq t \leq T_{Ph2} \quad (15)$$

$$y_{Ph2}(t) = Y_{ego} \left(-2.2 \left(\frac{t}{T_{Ph2}} \right)^3 + 3.2 \left(\frac{t}{T_{Ph2}} \right)^2 \right) \quad (16)$$

$$T_{Ph2} = TTC_1 - TTC_2 \quad (17)$$

2.7.2 Piecewise trajectory between point P2 and P3

During Phase 3, the ego vehicle's movement dictates a simpler trajectory compared to the initial turn (P1 to P2) for overtaking. While Phase 1 and 2 focus on the initial turn maneuver, Phase 3 (P2 to P3) involves maintaining a safe parallel distance alongside MC. The total duration of this straight movement is determined by the relative movement between the ego vehicle and MC including the previously established quantified driver comfort values for TTC_2 and TTC_3 . Eq. (18) - (20) are directly utilized within

control algorithms to ensure this safe parallel movement is maintained throughout Phase 3.

$$x_{Ph3}(t) = \frac{V_{ego}}{3.6} t, \quad 0 \leq t \leq T_{Ph3} \quad (18)$$

$$y_{Ph3}(t) = Y_{ego} \quad (19)$$

$$T_{Ph3} = TTC_2 + TTC_3 + \frac{L_{ego} + L_{mc}}{V_{ego} - V_{mc}} \quad (20)$$

2.7.3 Piecewise trajectory between point P3 and P4

Similar to the initial turn (P1 to P2), Phase 4 of the overtaking maneuver necessitates a controlled return to the original lane center. To achieve a smooth and comfortable lane re-entry trajectory, Eq. (8) was used to construct a piecewise trajectory between P3 and P4. This specific polynomial is detailed in Eq. (21) - (23). This approach prioritizes driver comfort during the final stage of the overtaking maneuver while ensuring a safe return to the designated lane.

$$x_{Ph4}(t) = \frac{V_{ego}}{3.6} t, \quad 0 \leq t \leq T_{Ph4} \quad (21)$$

$$y_{Ph4}(t) = Y_{ego} \left(2 \left(\frac{t}{T_{Ph4}} \right)^3 - 2.7 \left(\frac{t}{T_{Ph4}} \right)^2 - 0.2 \frac{t}{T_{Ph4}} + 1 \right) \quad (22)$$

$$T_{Ph4} = TTC_4 - TTC_3 \quad (23)$$

2.8. Overtaking Scenario Setup

The overtaking maneuvers were simulated on a virtual urban road with a left-hand traffic configuration, as depicted in Fig. 1. Both lanes were designed for unidirectional traffic, with each lane having a width W_l of 3 m. The MC dimensions were set to a width W_{mc} of 0.71 m and a length L_{mc} of 1.92 m. The ego vehicle, on the other hand, had a width W_{ego} of 1.8 m and a length L_{ego} of 4.9 m.

To analyze the effectiveness of the overtaking algorithm under diverse conditions that apply the Australian safety regulations for overtaking cyclists, the MC's lateral position Y_{mc} relative to the lane center was varied systematically. The position Y_{mc} ranged from -1 m (far left) to 1 m (far right) in increments of 1 m. The MC maintained a constant speed V_{mc} of 20 and 40 km/h throughout the simulations. The ego vehicle's speed V_{ego} was set to either 60 km/h or 80 km/h steady throughout the maneuvers, simulating different overtaking velocity differentials. This variation in the ego vehicle's speeds allows us to assess the algorithm's performance in scenarios relevant to the Australian safety guidelines for safe overtaking distances.

3. Results and Discussion

This section focuses on verifying the two key objectives of the trajectory planning algorithm through simulations using the FVRP planner: performance under various conditions and comparison with existing models.

The first objective is to validate the planner's ability to function effectively under different scenarios involving varying MC speeds, MC lateral positions, and ego vehicle speeds in aspects of trajectory, safety, psychological and physical comfort. The second objective involves comparing the FVRP planner's trajectory planning results with those generated by two established models: the driver behavior model and the optimal control model.

3.1. Evaluation of FVRP Trajectory Planning

Figures 9 and 10 illustrate the trajectory planning outcomes achieved using the FVRP concept for V_{mc} of 20 km/h and 40 km/h, respectively. Each graph depicts the trajectories of both the ego vehicle and the MC, highlighting their positions when they reach reference points P1 to P4. These results demonstrate the FVRP planner's capability to generate collision-free trajectories in all simulated conditions.

A critical aspect of the FVRP planner lies in its selection of the optimal lateral gap Gap_{Opt} between the ego vehicle and the MC. This selection process strives to strike a balance between driver comfort and established safety regulations. In Fig. 9a and 10a, a higher Gap_{Opt} values are chosen from Gap_{Lat} , resulting in larger lateral offsets for the ego vehicle Y_{ego} which are less than W_l of 3 m. This prioritizes driver comfort by creating a more spacious overtaking maneuver. However, in most other scenarios, the Gap_V plays a more significant role in determining Gap_{Opt} in Fig. 9b, 9d, 9e, 10b, 10d, and 10e. The lateral offset Y_{ego} values of those cases still stay within W_l of 3 m.

Consequently, the ego vehicle executes partial lane changes while maintaining a safe distance from the MC. In Fig. 9c, 9f, 10c, and 10f, prioritizing safety with higher Gap_V would have led to a Y_{ego} values exceeding W_l . To ensure safe operation and prevent the ego vehicle from exceeding lane boundaries, the planner automatically caps Y_{ego} at 3 m. This capping mechanism triggers full lane-change maneuvers for the ego vehicle, allowing it to safely overtake the MC within the lane's limitations.

Table 3 summarizes the total longitudinal distances traveled by the ego car ($D_{ego,tot}$) and MC ($D_{mc,tot}$) for the entire overtaking maneuver across all simulated conditions, along with the corresponding total maneuver times (T_{tot}). As expected, the total distances traveled by both the ego car $D_{ego,tot}$ and the MC $D_{mc,tot}$ were consistently higher for MC speeds of 40 km/h compared to 20 km/h. However, the increase of $D_{ego,tot}$ was minimal, while $D_{mc,tot}$ roughly doubled. These differences are directly attributable to the relative speed variations between the ego vehicle and the MC. The total maneuver times ranged from 12.3 s to 14.2 s across all scenarios.

Beyond the considerations of MC position and lane width discussed in Section 2.5, safe overtaking maneuvers in real-world scenarios necessitate sufficient headway in both the original and target lanes for successful completion, as shown in Table 3. If insufficient headway exists, the AV prioritizes following the MC. To ensure safety during overtaking, the AV should establish two crucial distances: pre-maneuver distance separating the AV from the MC before initiating the maneuver at P1 and post-maneuver following distance maintaining a safe

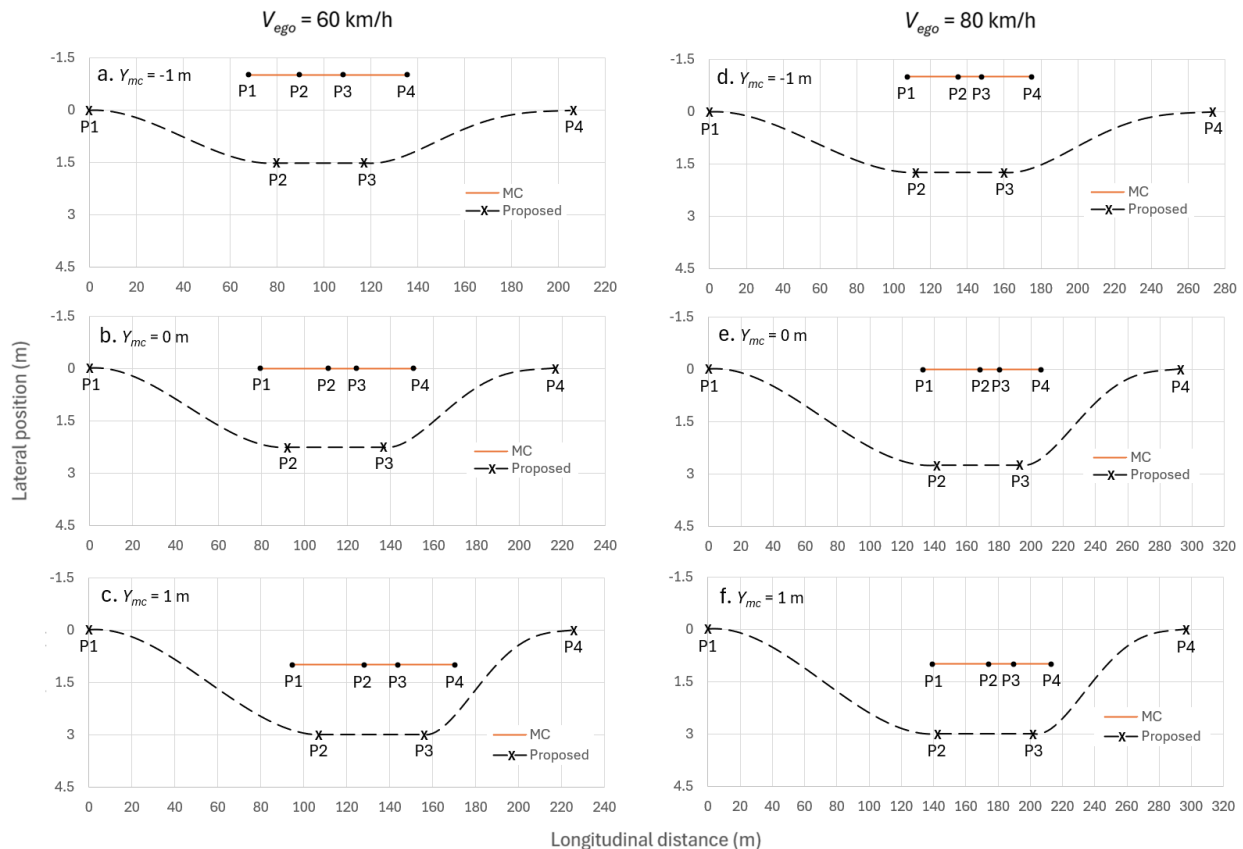


Fig. 9. Overtaking trajectories using FVRP at MC speed of 20 km/h.

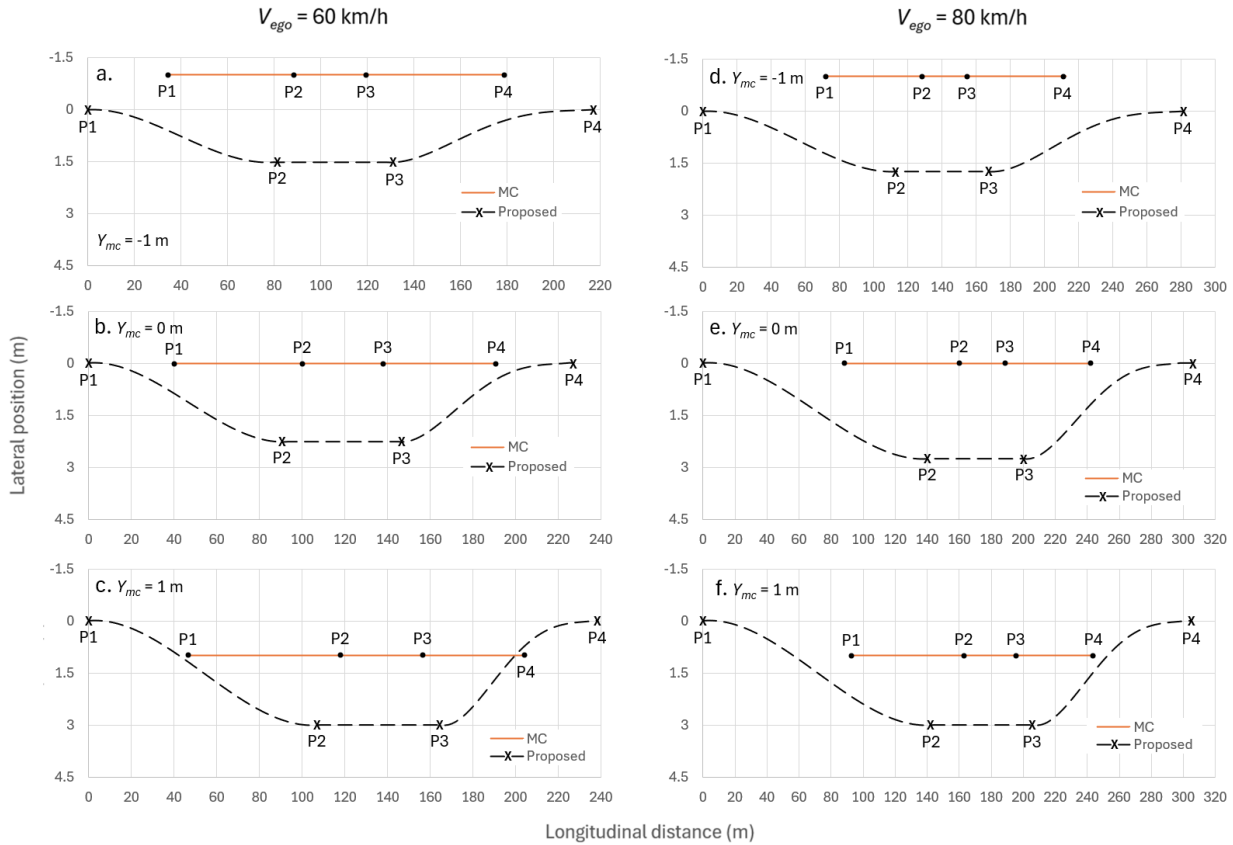


Fig. 10. Overtaking trajectories using FVRP at MC speed of 40 km/h.

following gap from any preceding vehicle after completing the lane change (e.g., the three-second rule [38]). The combined distance required for these maneuvers can reach nearly 400 m at an ego car speed of 80 km/h. However, typical long-range automotive radars used in advanced driver-assistance systems have a maximum detection range up to 250 m for objects directly in front of the vehicle [39]. This limitation necessitates the development of more capable long-range automotive radar systems with the ability to detect a vehicle in front through both sides of MC for proper overtaking planning and execution.

Table 4 analyzes the safety of overtaking trajectories generated by the FVRP concept against TTC and lateral gap criteria as listed in Table 1. The results demonstrate that FVRP effectively maintains safe headways throughout critical phases of the overtaking maneuver. Specifically, TTC_1 values, which represent TTC during the initial turn phase (Phase 1), consistently exceed 4 s, indicating a safe buffer zone. Similarly, TTC_3 values, which represent TTC during the cutting-in phase (Phase 4), remain above 0 s, ensuring safety during this crucial stage of overtaking. The most significant safety concerns arose regarding lateral gaps. FVRP generally adhered to the

Table 3. Total longitudinal distances and times of complete maneuver for ego car and MC for all simulated conditions.

Cases				$D_{ego,tot}$ (m)	$D_{mc,tot}$ (m)	T_{tot} (s)
Fig.	V_{ego} (km/h)	V_{mc} (km/h)	Y_{mc} (m)			
9a	60	20	-1	206	68	12.3
9b	60	20	0	216	72	13.0
9c	60	20	1	230	76	13.6
9d	80	20	-1	272	68	12.3
9e	80	20	0	287	73	13.2
9f	80	20	1	314	74	13.4
10a	60	40	-1	216	145	13.0
10b	60	40	0	226	151	13.6
10c	60	40	1	236	158	14.2
10d	80	40	-1	277	140	12.6
10e	80	40	0	292	149	13.4
10f	80	40	1	301	151	13.6

Table 4: Safety evaluation on FVRP trajectories

Cases			TTC_1 (s)		TTC_3 (s)		Gap_{opt} (m)	
V_{ego} (km/h)	V_{mc} (km/h)	Y_{mc} (m)	Criteria	Results	Criteria	Results	Criteria	Results
60	20	-1	≥ 4	6.1	≥ 0	0.4	≥ 1.0	1.26
60	20	0	≥ 4	7.2	≥ 0	0.4	≥ 1.0	1.00
60	20	1	≥ 4	8.3	≥ 0	0.4	≥ 1.0	<u>0.75</u>
80	20	-1	≥ 4	6.3	≥ 0	0.4	≥ 1.5	1.50
80	20	0	≥ 4	7.7	≥ 0	0.4	≥ 1.5	1.50
80	20	1	≥ 4	8.3	≥ 0	0.4	≥ 1.5	<u>0.75</u>
60	40	-1	≥ 4	6.1	≥ 0	0.4	≥ 1.0	1.26
60	40	0	≥ 4	7.2	≥ 0	0.4	≥ 1.0	1.00
60	40	1	≥ 4	8.3	≥ 0	0.4	≥ 1.0	<u>0.75</u>
80	40	-1	≥ 4	6.3	≥ 0	0.4	≥ 1.5	1.50
80	40	0	≥ 4	7.7	≥ 0	0.4	≥ 1.5	1.50
80	40	1	≥ 4	8.3	≥ 0	0.4	≥ 1.5	<u>0.75</u>

regulations, except in cases with Y_{mc} of 1 m. This discrepancy is likely caused by the limitation of keeping lateral offset Y_{ego} within the lane width of 3 m.

Driver physical comfort is also a crucial factor in evaluating autonomous driving behavior. The overtaking trajectories generated by the FVRP concept were implemented in CarSim software to simulate autonomous trajectory tracking. A path follower driver model in CarSim was employed within the simulation to control the ego vehicle's movement along the planned trajectory. During this simulation, the lateral acceleration experienced by the ego vehicle was collected. Literature [40] suggests that lateral accelerations around 1 m/s^2 are generally considered physically comfortable for human drivers under normal conditions.

Table 5 summarizes the maximum lateral accelerations ($a_{y,max}$) observed. In all scenarios, the maximum lateral acceleration values remained well below the 1 m/s^2 comfort threshold, indicating a comfortable driver experience throughout the overtaking maneuver. The peak lateral accelerations were similar for both MC speeds of 20 km/h and 40 km/h. This observation can be

Table 5. Maximum lateral accelerations observed on FVRP trajectories.

Cases			$a_{y,max}$ (m/s^2)	
V_{ego} (km/h)	V_{mc} (km/h)	Y_{mc} (m)	Criteria	Results
60	20	-1	1	0.04
60	20	0	1	0.06
60	20	1	1	0.08
80	20	-1	1	0.05
80	20	0	1	0.07
80	20	1	1	0.10
60	40	-1	1	0.04
60	40	0	1	0.06
60	40	1	1	0.08
80	40	-1	1	0.05
80	40	0	1	0.07
80	40	1	1	0.10

attributed to the fact that the peak lateral accelerations occurred during the returning phase (Phase 4), where the planned trajectories between Point P3 and P4 exhibited a similar shape for both speeds and were shorter compared to the trajectories between Point P1 and P2.

3.2. Comparison With Other Methods

The performance of FVRP concept was evaluated by comparing its results with two established models: a driver behavior model (DBM) based on Eq. (2) to (8) and an optimal control model (OCM) from [19] that minimizes total kinetic energy. Notably, the DBM and OCM can also be implemented within the four-phase overtaking framework.

To ensure a fair comparison, the OCM was configured specifically. It prioritized lateral gaps that considers Australian safety regulations while adhering to the W_l limitation for lateral offset Y_{ego} . This configuration also aligns with Australian safety guidelines for overtaking maneuvers. The comparison was done at V_{mc} of 40 km/h only. For a more balanced comparison, the longitudinal positions of points P2 and P3 were set at 0 s for both TTC_2 and TTC_3 in the OCM. This replicates the settings used in the original study [19], which focused solely on minimizing total kinetic energy during overtaking without incorporating driver behavior considerations. Finally, a maximum lateral acceleration of 1 m/s^2 (obtained from [40]) was used as a parameter for the OCM calculations.

Figure 11 compares the overtaking trajectories generated by the FVRP concept, DBM, and OCM. The FVRP and DBM trajectories exhibit a high degree of similarity, particularly in terms of overall path and timing. This suggests that the FVRP method effectively replicates natural driver behavior during overtaking maneuvers. However, some key differences emerge in the lateral offset Y_{ego} and the longitudinal distance TTC_3 during the ego vehicle's passing phase (Phase 3). Notably, the FVRP trajectories consistently maintain higher values for both Y_{ego} and TTC_3 . This prioritizes driver comfort by creating a larger lateral buffer between the ego vehicle and the MC,

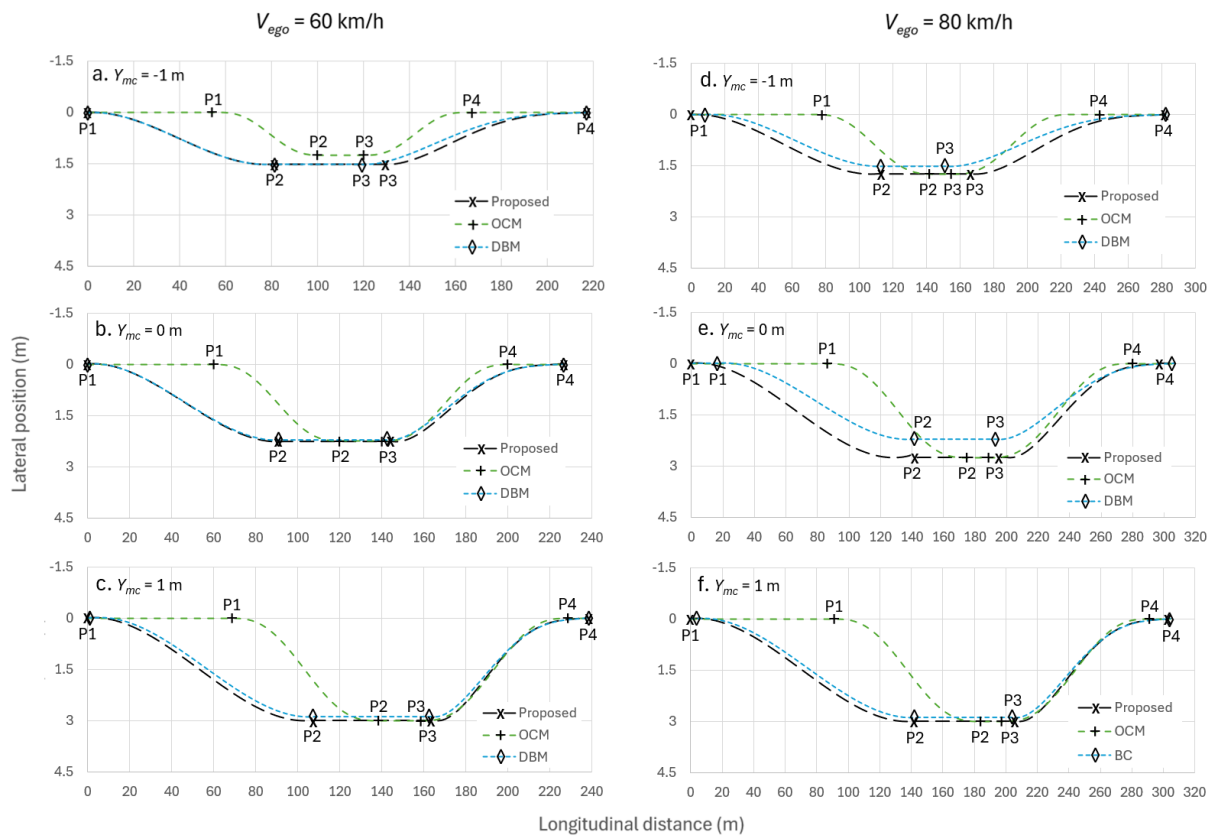


Fig. 11. Comparison of overtaking trajectories across three methods.

as well as allowing for a longer and potentially smoother overtaking maneuver during Phase 3.

In contrast, the OCM trajectories in Fig. 10 show significant deviations, particularly in their starting and ending points. The OCM maneuvers begin later and end earlier compared to the FVRP and DBM approaches. This difference can be attributed to the inherent asymmetry lane changing in human overtaking maneuvers. The OCM, on the other hand, prioritizes a more symmetrical approach, focusing solely on minimizing total kinetic energy, which may not always align with real-world driving behavior.

Table 7 summarizes the total longitudinal distances traveled by the ego car ($D_{ego,tot}$) and MC ($D_{mc,tot}$) across the three methods for the complete maneuver, along with the total maneuver times (T_{tot}). FVRP and DBM exhibited similar path lengths for both vehicles, while OCM prioritized efficiency consistently achieving both the shortest distances and time spending. Total maneuver

times generally decreased with increasing ego car speed except for OCM's T_{tot} , suggesting a complex interplay between speed, lateral positions, and OCM's control strategy.

Table 8 analyzes the safety of overtaking trajectories generated by the three methods against TTC and lateral gap criteria as listed in Table 1. FVRP and DBM maintained safe headways throughout Phase 1, with TTC_1 exceeding 4 s. Conversely, OCM exhibited lower TTC_1 values in some cases, potentially leading to collisions if an unforeseen event involving MC occurs. DBM displayed a safety limitation in specific scenarios ($Y_{mc} = -1$ m, $V_{ego} = 60$ and 80 km/h) with TTC_3 dropping below 0 s at the end of Phase 3. This highlights a potential risk of unsafe cutting-in behavior when relying solely on driver data.

The most significant safety concerns arose regarding lateral gaps. When compared to Australian safety regulations, DBM trajectories frequently violated these criteria due to inherent unsafe driver behavior patterns.

Table 7. Total longitudinal distances and times of complete maneuver for ego car and MC across three models.

Cases		FVRP			DBM			OCM		
V_{ego} (km/h)	Y_{mc} (m)	$D_{ego,tot}$ (m)	$D_{mc,tot}$ (m)	T_{tot} (s)	$D_{ego,tot}$ (m)	$D_{mc,tot}$ (m)	T_{tot} (s)	$D_{ego,tot}$ (m)	$D_{mc,tot}$ (m)	T_{tot} (s)
60	-1	217	145	13.0	217	145	13.0	110	73	6.6
60	0	226	151	13.6	225	150	13.5	140	93	8.4
60	1	237	158	14.2	235	157	14.1	160	107	9.6
80	-1	280	140	12.6	273	137	12.3	154	77	6.9
80	0	298	149	13.4	289	144	13.0	194	97	8.7
80	1	302	151	13.6	300	150	13.5	200	100	9.0

Table 8. Safety analysis on trajectories across three methods.

Cases		TTC_1 (s)			TTC_3 (s)			Gap_{opt} (m)					
V_{ego} (km/h)	Y_{mc} (m)	Criteria	FVRP	DBM	OCM	Criteria	FVRP	DBM	OCM	Criteria	FVRP	DBM	OCM
60	-1	4	6.1	6.1	<u>2.7</u>	0	0.4	<u>-0.2</u>	0	1	1.26	1.26	1.26
	0	4	7.2	7.1	<u>3.6</u>	0	0.4	0.1	0	1	1.00	<u>0.95</u>	1.00
	1	4	8.3	8.2	4.2	0	0.4	0.3	0	1	<u>0.75</u>	<u>0.64</u>	<u>0.75</u>
80	-1	4	6.3	6.1	<u>3.2</u>	0	0.4	<u>-0.2</u>	0	1.5	1.50	<u>1.26</u>	1.50
	0	4	7.7	7.1	4.0	0	0.4	0.1	0	1.5	1.50	<u>0.95</u>	1.50
	1	4	8.3	8.2	4.2	0	0.4	0.3	0	1.5	<u>0.75</u>	<u>0.64</u>	<u>0.75</u>

Both FVRP and OCM generally adhered to the regulations, except in cases with Y_{mc} of 1 m. This discrepancy is likely caused by the limitation of keeping lateral offset Y_{ego} within the lane width of 3 m.

Table 9 summarizes the results for maximum lateral acceleration obtained from the simulations. In all cases, the actual values remained below the 1 m/s² physical comfort threshold. Interestingly, FVRP and DBM trajectories yielded similar peak lateral accelerations, while OCM consistently produced the highest values. This difference can be attributed to OCM's shorter steering and lane return phases, resulting in more abrupt maneuvers.

The observed variations in maximum lateral acceleration between OCM and DBM in Table 9 suggest that overtaking trajectories might not be solely optimized for minimum total kinetic energy, which falls into the physical facet of car occupants. These findings align with previous research [17], which suggests that drivers might rely more on psychological factors and visual cues during overtaking maneuvers. These factors can include various parameters like headway distances, obstacle proximity during braking, and vehicle speed. This emphasizes the importance of incorporating driver behavior patterns into trajectory planning algorithms for autonomous vehicles.

The proposed FVRP concept demonstrates several advantages over the other two models in achieving a balance between the safety and driver psychological comfort distances during overtaking maneuvers. Unlike the other models that might prioritize one aspect over the other, FVRP integrates both factors from the very beginning of the planning process. This is achieved by incorporating quantified driver psychological comfort zone data into the FVRP framework. This data allows the

Table 9. Maximum lateral accelerations on trajectories across three methods.

Cases		$a_{y,max}$ (m/s ²)			
V_{ego} (km/h)	Y_{mc} (m)	Criteria	FVRP	DBM	OCM
60	-1	1	0.04	0.04	0.06
60	0	1	0.06	0.06	0.07
60	1	1	0.08	0.08	0.11
80	-1	1	0.05	0.04	0.08
80	0	1	0.07	0.06	0.09
80	1	1	0.10	0.09	0.11

algorithm to adapt in situations where the safety and psychological comfort objectives might conflict. As a result, the FVRP concept can generate overtaking trajectories that prioritize safety while still considering driver psychological comfort preferences. Furthermore, the FVRP concept has the potential for broader applicability in car-MC overtaking scenarios beyond the situations considered in this study. For instance, the framework could be adapted to address overtaking maneuvers when MC is parked at the outermost lane or brakes in both the innermost and outermost lanes, as observed in [23].

In contrast, DBM and some Artificial Neural Network (ANN) approaches like in literature [7-9] rely solely on driver data, which may contain inherent unsafe behaviors, especially in complex maneuvers as noted in [24, 42]. Modifying such data to eliminate these risks can be challenging. While some studies attempt to address this by training ANNs with pre-screened safe driving data [8], the resulting data set might be insufficient for robust training. Additionally, OCM, solely focused on minimizing total kinetic energy, lacks the ability to directly incorporate the safety and psychological comfort considerations without the traffic safety criteria and driver data.

Despite its advantages, the FVRP approach has some potential drawbacks. Firstly, the reliance on average driver data might result in trajectories that deviate from individual preferences. This can occur due to the inherent differences between averaged comfort zones and those of specific users, potentially leading to discomfort and reduced trust in the AV as noted in [5]. Modifying trajectories to meet individual needs can also be challenging for ordinary users, as it might require a deep understanding of the overtaking maneuver itself. Additionally, user-requested modifications might sometimes violate safety constraints, which cannot be compromised.

The FVRP concept's reliance on driver data for quantifying comfort zone preferences presents a crucial drawback. This data can exhibit significant variations across different regions and countries due to several factors such as variations between left-hand and right-hand traffic configurations, lane widths, the total number of lanes, etc. As also highlighted in [24], driver behavior during overtaking maneuvers can differ substantially between countries like Japan and Thailand. Consequently, the overtaking trajectories generated in this study, based on a

dataset collected from a sample of Thai drivers, might not be directly applicable in other countries. This necessitates new data collection efforts specific to the target region or country for deployment of the FVRP concept. Furthermore, the FVRP approach, currently focused on overtaking maneuvers, might require adaptation for broader applicability in various driving maneuvers beyond overtaking.

3.3. Limitations of This Study

This study acknowledges several limitations that present opportunities for future research. These limitations are discussed as follows.

- The model relies on predefined rules and parameters, limiting its adaptability to unseen scenarios or variations in driving conditions.

- The model's reliance on pre-defined reference points might restrict its ability to respond dynamically to real-time changes in traffic conditions such as swerving maneuvers by MC.

- While the model incorporates some aspects of driver behavior, it does not fully capture the complexities and variations in human decision-making.

- The model's performance relies on several assumptions, such as the accuracy of the initial model parameters such as MC size and the consistency of driver behavior.

- The effects of encountering multiple MCs during overtaking maneuvers.

- The effects of other vehicles present in the scene on the overtaking behavior.

- The impact of narrower road lanes on overtaking strategies.

There are several techniques and methods to address the limitations of the model presented in this study. Here are some potential approaches:

- Hybrid Approach by integrating the rule-based model with machine learning techniques to leverage the strengths of both approaches. For example, use machine learning to refine model parameters or to handle unexpected scenarios.

- Utilize advanced sensor fusion techniques to improve the model's perception of the environment. By combining data from multiple sensors, the model can better anticipate and respond to dynamic situations.

- Incorporate driver models that capture individual differences in driving behavior to improve the model's generalizability. This can be achieved through clustering or personalization techniques.

4. Conclusions

This research introduces the FVRP framework for generating human-like and safe overtaking trajectories for AVs in car-MC overtaking scenarios. By decomposing the complex overtaking maneuver into distinct phases and defining virtual reference points based on driver psychological comfort and safety considerations, the

FVRP approach offers a structured method for trajectory planning. This framework integrates elements of engineering, psychology, and human-computer interaction to create a more naturalistic and safe overtaking strategy for AVs.

Compared to existing methods like DBM and OCM, FVRP offers distinct advantages. It can preserve human driver characteristics, such as asymmetric lane-change maneuvers and partial lane-change behaviors, while maintaining the flexibility to prioritize safety by replacing comfort distances with stricter safety constraints when necessary.

The effectiveness of the proposed FVRP algorithm in real-world overtaking scenarios is influenced by several factors that necessitate further refinement. These challenges include the presence and behavior of other MCs and vehicles, unpredictable swerving maneuvers by MC riders, variations in MC size due to modifications or cargo, and narrow lane widths.

References

- [1] L. Oliveira, K. Proctor, C. G. Burns, and S. Birrell, "Driving style: How should an automated vehicle behave?," *Information*, vol. 10, no. 6, pp. 219, 2019.
- [2] B. Paden, M. Čáp, S. Z. Yong, D. Yershov, and E. Frazzoli, "A survey of motion planning and control techniques for self-driving urban vehicles," *IEEE Transactions on Intelligent Vehicles*, vol. 1, no. 1, pp. 33-55, 2016.
- [3] S. Dixit, S. Fallah, U. Montanaro, M. Dianati, A. Stevens, F. Mccullough, and A. Mouzakitis, "Trajectory planning and tracking for autonomous overtaking: State-of-the-art and future prospects," *Annual Reviews in Control*, vol. 45, pp. 76-86, 2018.
- [4] H. Zheng, J. Zhou, Q. Shao, and Y. Wang, "Investigation of a longitudinal and lateral lane-changing motion planning model for intelligent vehicles in dynamical driving environments," *IEEE Access*, vol. 7, pp. 44783-44802, 2019.
- [5] C. Dai, C. Zong, D. Zhang, G. Li, K. Chuyo, H. Zheng, and F. Gao, "Human-like lane-changing trajectory planning algorithm for human-machine conflict mitigation," *Journal of Intelligent and Connected Vehicles*, vol. 6, no. 1, pp. 46-63, 2023.
- [6] N. Naidja, S. Font, M. Revilloud, and G. Sandou, "An interactive game theory-PSO based comprehensive framework for autonomous vehicle decision making and trajectory planning," in *22nd World Congress of the International Federation of Automatic Control*, 2023.
- [7] J. Zhao, D. Song, B. Zhu, Z. Sun, J. Han, and Y. Sun, "A human-like trajectory planning method on a curve based on the driver preview mechanism," *IEEE Transactions on Intelligent Transportation Systems*, vol. 24, no. 11, pp. 11682-11698, 2023.
- [8] J. Nan, W. Deng, R. Zhang, Y. Wang, R. Zhao, and J. Ding, "Interaction-aware planning with deep inverse reinforcement learning for human-like

- autonomous driving in merge scenarios,” *IEEE Transactions on Intelligent Vehicles*, vol. 9, no. 1, pp. 2714-2726, Jan. 2024.
- [9] J. Liu, X. Qi, Y. Ni, J. Sun, and P. Hang, “Teaching autonomous vehicles to express interaction intent during unprotected left turns: A human-driving-prior-based trajectory planning approach,” 2023, *arXiv:2307.15950*.
- [10] B. Fajen and A. J. Jansen, “Steering through multiple waypoints without model-based trajectory planning,” *Journal of Vision*, vol. 23, no. 9, pp. 5019-5019, 2023.
- [11] M. Cui, Y. Hu, S. Xu, J. Wang, Z. Bing, B. Li, and A. Knoll, “Safe and human-like trajectory planning of self-driving cars: A constraint imitative method,” *Advanced Intelligent Systems*, vol. 5, no. 10, p. 2300269, 2023.
- [12] X. Chen, W. Zhang, H. Bai, C. Xu, H. Ding, and W. Huang, “Two-dimensional following lane-changing (2DF-LC): A framework for dynamic decision-making and rapid behavior planning,” *IEEE Transactions on Intelligent Vehicles*, vol. 9, no. 1, pp. 427-445, Jan. 2023.
- [13] G. Abe, K. Sato, and M. Itoh, “Driver trust in automated driving systems: The case of overtaking and passing,” *IEEE Transactions on Human-Machine Systems*, vol. 48, no. 1, pp. 85-94, 2017.
- [14] Y. Chen and J. Wang, “Personalized vehicle path following based on robust gain-scheduling control in lane-changing and left-turning maneuvers,” in *2018 Annual American Control Conference*, 2018, pp. 4784-4789.
- [15] E. Dumur, Y. Barnard, and G. Boy, “Designing for comfort,” *Human Factors in Design*, pp. 111-127, 2004.
- [16] C. Sèze, *Confort moderne: une nouvelle culture du bien-être*. Paris: Autrement, 1994.
- [17] M. Elbanhawi, M. Simic, and R. Jazar, “In the passenger seat: investigating ride comfort measures in autonomous cars,” *IEEE Intelligent Transportation Systems Magazine*, vol. 7, no. 3, pp. 4-17, 2015.
- [18] K. Chu, M. Lee, and M. Sunwoo, “Local path planning for off-road autonomous driving with avoidance of static obstacles,” *IEEE Transactions on Intelligent Transportation Systems*, vol. 13, no. 4, pp. 1599-1616, 2012.
- [19] T. Shamir, “How should an autonomous vehicle overtake a slower moving vehicle: Design and analysis of an optimal trajectory,” *IEEE Transactions on Automatic Control*, vol. 49, no. 4, pp. 607-610, 2004.
- [20] S. Hecker, D. Dai, and L. Van Gool, “Learning accurate, comfortable and human-like driving,” 2019, *arXiv: 1903.10995*.
- [21] Y. Morales, N. Kallakuri, K. Shinozawa, T. Miyashita, and N. Hagita, “Human-comfortable navigation for an autonomous robotic wheelchair,” in *IEEE/RISJ International Conference on Intelligent Robots and Systems*, 2013, pp. 2737-2743.
- [22] H. Farah, G. B. Piccinini, M. Itoh, and M. Dozza, “Modelling overtaking strategy and lateral distance in car-to-cyclist overtaking on rural roads: A driving simulator experiment,” *Transportation Research Part F: Traffic Psychology and Behaviour*, vol. 63, pp. 226-239, 2019.
- [23] G. Panero, “Drivers’ comfort zone boundaries when overtaking pedestrians—Analysis of naturalistic driving and field test data,” Master thesis, Chalmers University of Technology, Göteborg, Sweden, 2018.
- [24] S. Sitthiracha, S. Koetniyom, and G. Phanomchoeng, “Modeling of car-to-motorcycle overtaking maneuver based on comfort zone boundaries,” *Applied Science and Engineering Progress*, vol. 17, no. 3, 2024.
- [25] E. Hollnagel and D. D. Woods, *Joint Cognitive Systems: Foundations of Cognitive Systems Engineering*. CRC Press, 2005.
- [26] J. Engström and E. Hollnagel, “A general conceptual framework for modelling behavioural effects of driver support functions,” in *Modelling Driver Behaviour in Automotive Environments: Critical Issues in Driver Interactions with Intelligent Transport Systems*. Springer, 2007.
- [27] M. Ljung Aust and J. Engström, “A conceptual framework for requirement specification and evaluation of active safety functions,” *Theoretical Issues in Ergonomics Science*, vol. 12, no. 1, pp. 44-65, 2011.
- [28] J. A. Michon, “A critical view of driver behavior models: what do we know, what should we do?,” in *Human Behavior and Traffic Safety*. Boston, MA: Springer US, 1985.
- [29] H. Summala, “Towards understanding motivational and emotional factors in driver behaviour: Comfort through satisficing,” in *Modelling Driver Behaviour in Automotive Environments: Critical Issues in Driver Interactions with Intelligent Transport Systems*. Springer, 2007, pp. 189-207.
- [30] R. Fuller, “Driver control theory: From task difficulty homeostasis to risk allostasis,” in *Handbook of Traffic Psychology*. Academic Press, 2011.
- [31] T. Vaa, “Drivers’ information processing, decision-making and the role of emotions: Predictions of the Risk Monitor Model,” in *Human Modelling in Assisted Transportation: Models, Tools and Risk Methods*. Springer Milan, 2011.
- [32] K. Czarnecki, “Automated driving system (ads) task analysis-part 2: structured road maneuvers,” Waterloo Intelligent Systems Engineering Lab Report, University of Waterloo, 2018.
- [33] L. X. Li and P. H. Li, “Analysis of driver's steering behavior for lane change prediction,” in *11th International Conference on Intelligent Human-Machine Systems and Cybernetics*, IEEE, 2019.
- [34] R. Van Der Horst and J. Hogema, “Time-to-collision and collision avoidance systems,” in *Proc. 6th ICTCT Workshop*, Salzburg, 1993.
- [35] S. Hirst and R. Graham, “The format and presentation of collision warnings,” in *Ergonomics and Safety of Intelligent Driver Interfaces*. USA: CRC Press, 1997.

- [36] J. R. R. Mackenzie, J. K. Dutschke, and G. Ponte, "An evaluation of bicycle passing distances in the ACT," University of Adelaide, Adelaide, Australia, CASR157, 2019.
- [37] T. Liu, C. Wang, R. Fu, Y. Ma, Z. Liu, and T. Liu, "Lane-change risk when the subject vehicle is faster than the following vehicle: A case study on the lane-changing warning model considering different driving styles," *Sustainability*, vol. 14, no. 16, p. 9938, 2022.
- [38] D. R. King, K. B. Phillips, and D. A. Krauss, "Knowledge of state-recommended following-distance rules," in *Proceedings of the Human Factors and Ergonomics Society Annual Meeting, 2022*, vol. 66, no. 1, pp. 878-882.
- [39] R. Zheng, S. Sun, W. Kuo, T. Abatzoglou, and M. Markel, "4D automotive radar exploiting sparse array optimization and compressive sensing," in *57th Asilomar Conference on Signals, Systems, and Computers*, IEEE, 2023.
- [40] N. H. Gartner, C. J. Messer, and A. Rathi, *Traffic Flow Theory—A State-of-the-Art Report: Revised Monograph on Traffic Flow Theory*. 2002.
- [41] S. Sitthiracha, S. Koetniyom, K. Tontiwattanakul, G. Phanomchoeng, and S. Chantranuwathana, "Understanding driver's maneuver for passing a motorcycle on urban multi-lane road: Thailand case study," SSRN 4213504.
- [42] F. Sagberg, S. Selpi, G. F. Bianchi Piccinini, and J. Engström, "A review of research on driving styles and road safety," *Human Factors: The Journal of the Human Factors and Ergonomics Society*, vol. 57, no. 7, pp. 1248–1275, 2015.



Sitthichok Sitthiracha, photograph and biography not available at the time of publication.

Chinnawut Nantabut, photograph and biography not available at the time of publication.

Saiprasit Koetniyom, photograph and biography not available at the time of publication.

Gridsada Phanomchoeng, photograph and biography not available at the time of publication.